Coherent photon radiation from nuclei as a probe of impact-parameter and nucleon-velocity distribution in ultrarelativistic nuclear collisions

James D. Bjorken and Larry McLerran
Fermi National Accelerator Laboratory, P.O. Box 500, Batavia, Illinois 60510
(Received 20 August 1984)

Photons which are coherently produced when nucleons are accelerated during the collisions of ultrarelativistic nuclei are studied as probes of the impact parameter of the collision and of the rapidity distribution of the recoil nucleons.

I. INTRODUCTION

In the collisions of ultrarelativistic nuclei, the individual nucleons within the nuclei undergo tremendous accelerations. Those accelerated nucleons which are charged will radiate photons. Since there are a large number of charged nucleons in the nuclei, this photon radiation is greatly enhanced if it is coherent. Such coherent photon radiation should have strength $Z^2\alpha/\pi$, where Z is the number of nucleons which become accelerated. This relation is valid if the final velocities of the accelerated nucleons are not too close to the velocity of light. Otherwise, there may be a large numerical coefficient which grows in magnitude as the speed of light is approached. The condition for coherence is that in the rest frame of each of the nuclei, the photons have wavelengths longer than the nuclear diameter. In this circumstance, all of the accelerated nucleons may contribute to the amplitude for photon emission. The number of accelerated nucleons of course depends upon the impact parameter of the collision, and is measured by the total number of emitted photons above an infrared cutoff frequency. Therefore, if the soft photons can be observed in individual events, the impact parameter for an ion-ion collision can be determined on an event-by-event basis in a fairly model-independent way. Another quantity that may be extracted from measurements of the total number of photons and their angular distribution is the final velocity distribution of the accelerated nucleons. If all the nucleons were accelerated from rest to a fixed velocity v, the bulk of the photon radiation would be emitted in a cone at an angle of $1/2\gamma$ relative to the direction of the velocity vector. Here γ is the Lorentz boost factor for the velocity v. The total number of photons will also exhibit some dependence on the velocity v, which is fairly weak if γ is not too large.

The total number of detectable photons depends on the infrared-cutoff frequency. In the rest frame of the nucleus before acceleration, which we shall call the target rest frame, this cutoff might be as small an energy as 10 keV or perhaps as high as 1 MeV, depending on the detector used, the magnitudes of various backgrounds, and the characteristics of the collision geometry (e.g., colliding beams vs fixed target). At very high frequencies photons emitted from decays of hadrons produced in the nuclear collision may obscure a signal. The background arising from the decays of π^0 mesons will probably first obscure this signal as the frequency is increased. We shall show in a later section that this background becomes important for photon energies $E>15$ MeV. For energies $E<15$ MeV, the photons are coherent since $E\ll\pi/D\sim40$ MeV, where D is the nuclear diameter (taken to be $D\sim15$ fm for uranium). For such small energies there may be backgrounds due to photons produced from nuclear disintegration. We do not expect that these photons will be a significant background for central nuclear collisions. There may conceivably be "backgrounds" from photon emission arising from the hot quark-gluon plasma, a phenomenon which is a primary motivation for the experiment. However, one expects such contributions to be predominant at larger photon energies. At such low photon energies as considered here, low-energy theorems should require a suppression of contributions from local charge fluctuations. In any case the Z dependence (proportional to Z^2) and the angular distribution of the signal from a plasma should provide a ready means of discriminating the soft bremsstrahlung photons of interest here from plasma photons.

The differential energy spectrum of emitted photons has the soft photon divergence of $dN/d\omega\sim1/\omega$. The total number of emitted photons should be approximately

$$N\sim Z^2\frac{\alpha}{\pi}\ln\frac{\omega_{\max}}{\omega_{\min}} \tag{1}$$

so long as the typical γ factor of the accelerated nucleons is $\gamma\sim1$–2. Taking, in the target rest frame, $\omega_{\max}\sim15$ MeV and $\omega_{\min}$ as 1 MeV or 10 keV, the total number of emitted photons becomes 10–100 photons or 50–500 photons for head-on collisions of heavy nuclei with $Z\sim100$. The minimal detectable photon energy on which this result depends cannot be more strictly limited without better knowledge of specific detector systems and accelerator designs. Notice that for a collider, these photon frequencies become Doppler shifted by a factor of γ. For a 30-GeV/nucleon collider, these energies are $\omega_{\max}\sim0.5$ GeV and $\omega_{\min}\sim30$ MeV or 300 keV. For a fixed-target experiment with a projectile nucleus of 200 GeV/nucleon, the projectile nucleus radiates detectable photons with frequencies in the range 200 MeV$-$2 MeV $<\omega<3$ GeV.

In this paper we analyze photon emission from accelerated nucleons produced in nucleus-nucleus collisions. Much of the work presented is a generalization and refinement to ultrarelativistic nuclear collisions of the work of Kapusta[1] which was specifically tailored to Bevalac energies.[2] We shall consider the effects of a velocity distribution of nucleons, which smears out the simpler pattern produced assuming uniform velocities of the final-state nucleons. We shall describe how this velocity distribution might be inferred from measurements of the angular distributions of photons. We shall also describe how the impact parameter might be extracted from measurements of the total number of produced photons. We shall also estimate the background due to photons from π^0 decays, and determine for which energies the signal dominates this background for various values of Z.

II. THE PHOTON DISTRIBUTION

The computation of the frequency distribution of soft photons from an accelerated charge distribution may be done using classical electromagnetic theory. An essential ingredient in this computation is the space-time picture of the acceleration process. In Fig. 1, the collision of the two nuclei is viewed in the rest frame of the target nucleus. The projectile nucleus appears as a Lorentz-contracted pancake which uniformly accelerates the charges. These charges are sequentially accelerated as the projectile nucleus sweeps through the target. In our analysis, we shall ignore the transverse acceleration of the nucleons since the average over all nucleons of such acceleration is small and will not lead to significant coherent radiation.

The distribution of radiation from an accelerated charge distribution is[3]

$$\frac{d^2N}{d\omega\, d\Omega}=\frac{\alpha\omega}{4\pi^2}\left|\int d^4x\, \vec{n}\times[\vec{n}\times\vec{J}(x)]e^{i\omega(t-\vec{n}\cdot\vec{x})}\right|^2 . \quad (2)$$

The unit vector $\vec{n}$ is in the direction of the emitted photon's momentum. The current which contributes to this expression may be found from the space-time picture of Fig. 1,

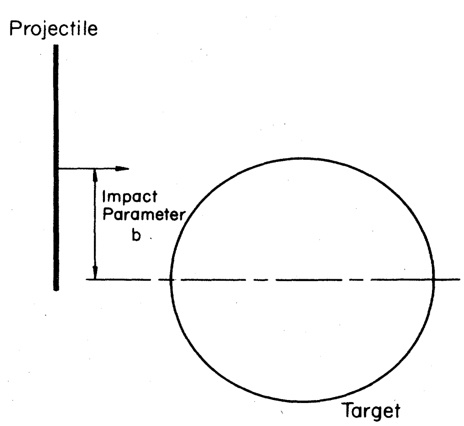

FIG. 1. The projectile nucleus sweeping through the target nucleus and accelerating the target nucleons.

$$\vec{J}(\vec{x},t)=\frac{Z}{V}\int_{V'}d^3x'\int dy\frac{dN}{dy}\delta^{(3)}(\vec{x}-\vec{x}\,'-\vec{v}(y)(t-x_3))$$

$$\times\vec{v}(y)\theta(t-x_3) . \quad (3)$$

The overlap volume of these two nuclei at impact parameter b is denoted by V' and the volume of each of the two equal-size nuclei is V. The step function arises because the projectile nucleus is Lorentz contracted down to a thickness which is very small compared to the wavelength of the emitted radiation. In Eq. (3), the target nucleus is centered at $\vec{r}=0$, and polar angles will be measured relative to the collision axis with $\theta=0$ corresponding to photon emission in the direction of the projectile beam.

The velocities of the struck nucleons are distributed according to a normalized rapidity distribution function dN/dy, where

$$v=\tanh y \quad (4)$$

and

$$1=\int dy\frac{dN}{dy} . \quad (5)$$

This distribution of velocities will be taken to be independent of transverse radius and impact parameter, an approximation which should be fair for the bulk of the nucleons in a head-on collision. This approximation is perhaps not as good for impact parameter $b\neq0$ collisions where there is a large asymmetry between target and projectile, and where the thickness of the two nuclei is varying fairly rapidly in the overlap region where they collide. Fortunately, most of the cross section for bremsstrahlung photon production comes for near head-on collisions.

We are also assuming that the distribution of nucleon velocities is one-dimensional,

$$\vec{v}=v\hat{e}_3 . \quad (6)$$

The transverse velocities acquired by the nucleons will average to zero for collisions with impact parameter zero. For nonzero-impact-parameter collisions there may be some small net transverse momentum in the target, but we do not expect large coherent photon emission in the transverse direction.

Finally, when the distribution functions for the probability for producing nucleons of rapidity y appear in the expression for the current, we are implicitly assuming that quantum-mechanical interference effects involving the hadronic wave functions are unimportant during the time of emission of the photons. We are, of course, allowing for the interference of the electromagnetic waves which are emitted from these nucleons. This approximation should be valid since the photon-emission time for low-frequency photons is large compared to natural scattering times.

Using Eqs. (2) and (3), the distribution of photons becomes

$$\frac{d^2N}{d\omega\, d\Omega}=\frac{Z^2\alpha}{4\pi^2}\omega \sin^2\theta \left| \frac{1}{V}\int d^3x' \int dy \int_{x_3'}^{\infty} dt \frac{dN}{dy} v(y) e^{i\omega t[1-v(y)\cos\theta]} e^{i\omega v(y)x_3'} e^{-i\omega \vec{n}\cdot\vec{x}} \right|^2 . \qquad (7)$$

Integrating over time gives

$$\frac{d^2N}{d\omega\, d\Omega}=\frac{Z^2\alpha}{4\pi^2 V\omega} \left| \int dy \frac{dN}{dy} \int_{V'} d^3x' \frac{v(y)\sin\theta}{1-v(y)\cos\theta} e^{i\omega(x_3'-\vec{n}\cdot\vec{x}')} \right|^2 . \qquad (8)$$

For soft photons, $\omega \ll \pi/D$, the phase variation in Eq. (8) is unimportant, and we have

$$\frac{d^2N}{d\omega\, d\Omega}=\frac{Z_{\rm eff}{}^2\alpha}{4\pi^2\omega} |g(\theta)|^2 . \qquad (9)$$

$Z_{\rm eff}$ is the number of charged particles which are in the overlap collision region, that is, the number of target nucleons which become accelerated. The angular distribution function which arises from the smearing over nucleon rapidities is

$$g(\theta)=\int dy \frac{dN}{dy}\frac{v(y)\sin\theta}{1-v(y)\cos\theta} . \qquad (10)$$

Notice that for a δ-function rapidity distribution corresponding to a velocity v, we obtain

$$|g(\theta)|^2=\frac{v^2\sin^2\theta}{(1-v\cos\theta)^2} \qquad (11)$$

which is the result for a point particle instantaneously accelerated from rest to velocity v. This is the result of Kapusta.[1]

A simple feature of this result is the factorization into a factor, $Z_{\rm eff}{}^2$, which measures the impact parameter, and a factor, $|g(\theta)|^2$, which measures the velocity distribution. Since the first factor reflects the total cross section, and the second factor determines the angular distribution, these factors are easy to separate.

The computation of $Z_{\rm eff}$ involves a simple geometrical overlap integral

$$\frac{Z_{\rm eff}}{Z}=\frac{1}{V}\int d^3x\, \theta(R^2-x^2-y^2-z^2) \times \theta[R^2-y^2-(z-b)^2] . \qquad (12)$$

A plot of $Z_{\rm eff}/Z$ is shown in Fig. 2.

The angular distribution function $g(\theta)$ is determined by the rapidity distribution dN/dy of struck nucleons. To model this dependence, we consider a rapidity distribution which interpolates between the distribution characteristic of pp interactions, e^{-y}, and a uniform rapidity distribution,

$$\frac{dN}{dy}=e^{-ay} . \qquad (13)$$

The fractional energy loss of a nucleon (in the projectile frame) for this distribution is

$$f=\frac{1}{(a+1)} . \qquad (14)$$

The computation of $g(\theta)$ for this rapidity distribution is carried out in Appendix A. The result is

$$g(\theta)=\sin\theta\left[\frac{1}{(a-2)}{}_2F_1\left[1,2;2-\frac{a}{2};\frac{1-\cos\theta}{2}\right] +(1-\cos\theta)^{a/2-1}2^{-a/2-1}\frac{a\pi}{\sin(a\pi/2)} + {}_2F_1\left[\frac{a}{2},\frac{a}{2}+1;\frac{a}{2};\frac{1-\cos\theta}{2}\right]\right] . \qquad (15)$$

This distribution has a singularity at $\theta=0$ if $a>1$. The strength of this singularity is

$$\lim_{\theta\to 0} g(\theta)=\frac{a\pi}{2^a\sin(a\pi/2)}\theta^{a-1} \qquad (16)$$

and can be shown to only depend upon the form of the rapidity distribution for large y. A plot of $|g(\theta)|^2$ is shown in Fig. 3, and the singular behavior for different a values is clearly exhibited.

A measure of the experimental requirements in extracting $g(\theta)$ is provided by the integral distribution of photons produced with angles $>\theta$ (in the target frame)

$$h(\theta)=\int_{\pi}^{\theta} d\theta' \sin\theta' |g(\theta')|^2 . \qquad (17)$$

Plots of the normalized integral distribution $R(\theta)=h(\theta)/h(0)$ are shown in Fig. 4 for the laboratory frame as well as for emissions from nuclei with Lorentz γ factors corresponding to 30 GeV/nucleon and 200 GeV/nucleon. These last two values are appropriate for proposed colliding-beam experiments and fixed-target ex-

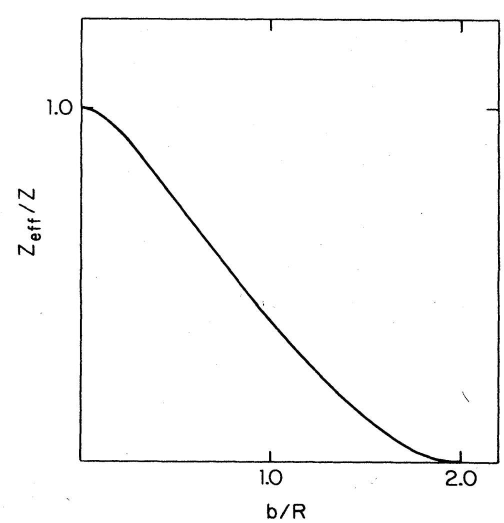

FIG. 2. The ratio $Z_{\rm eff}/Z$.

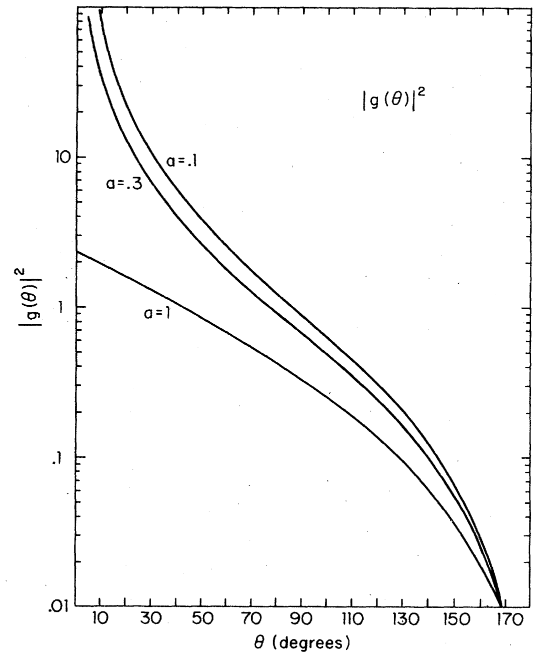

FIG. 3. The angular-distribution function for various values of the parameter a.

periments at the CERN SPS. In the laboratory frame, the typical emission angle is 50° for $a=1$, 35° for $a=\frac{1}{2}$, and 5° for the extreme case where $a=\frac{1}{10}$. For $\gamma=30$, these angles are 0.9, 0.55, and 0.01 degrees. For $\gamma=200$, the angles become 0.14, 0.07, and 0.005 degrees.

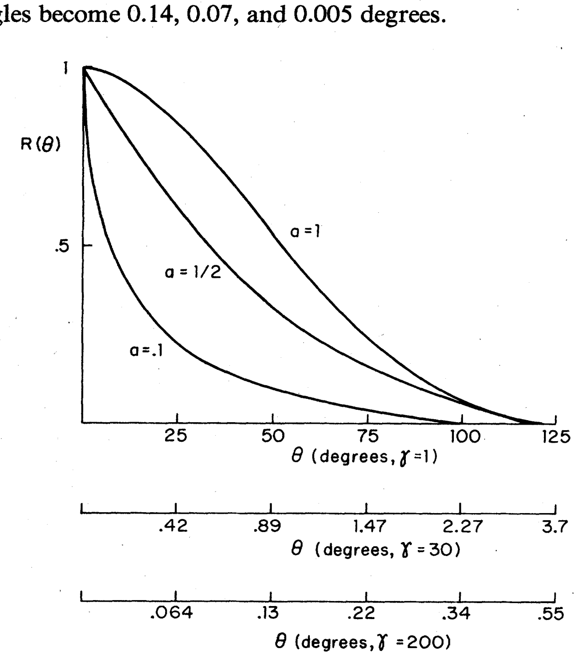

FIG. 4. The integral angular-distribution function $R(\theta)$ for various values of a and various values of initial nucleon momenta. The lower scales refer to Lorentz γ values of the nuclei which produce the photons of $\gamma=1$ corresponding to the target rest frame, of $\gamma=30$ corresponding to a collider, and $\gamma=200$ corresponding to a fixed-target energy appropriate to the SPS.

III. TOTAL YIELDS AND BACKGROUNDS

The total yield of photons may be computed from Eq. (8), assuming a value for the cutoff energies and for an impact parameter. In Fig. 5, the yield for impact-parameter-zero collisions given cutoff energies of $E=1$ MeV and 10 keV are plotted for $Z=90$ and $Z=57$. The values of a chosen are 0.1—1.0. Reasonable values probably lie in the range between $a=0.3$ and $a=1$. For $Z=90$ and $E=1$ MeV, the range of photon yields is 25—100 photons. For the lower energy cutoff, this number becomes 60—350 photons. For $Z=57$, these yields are reduced by a factor of 2.

If the photon yields are in the range of about 100 photons, it should be possible to discriminate impact parameters with some reliability. In any case if the signal exceeds backgrounds from decays of π^0 mesons, the angular distribution of the photons gives information on the nucleon-velocity distribution.

The distribution of soft background photons is easily estimated given the distribution of π^0 mesons. In Appendix B a derivation of the first-order corrections to the results we derive in this section will be presented, as well as further details of the derivation presented here. The distribution of π^0 mesons is assumed to be (in the projectile frame)

$$\frac{dN^\pi}{d^3p}=\frac{1}{E}F(x)g(p_T)\ , \tag{18}$$

where x is the fractional center-of-mass momentum. In the laboratory frame this becomes

$$\frac{dN^\pi}{d^3p}=\frac{1}{E}F\left[\frac{E-p}{M_p}\right]g(p_T)\ . \tag{19}$$

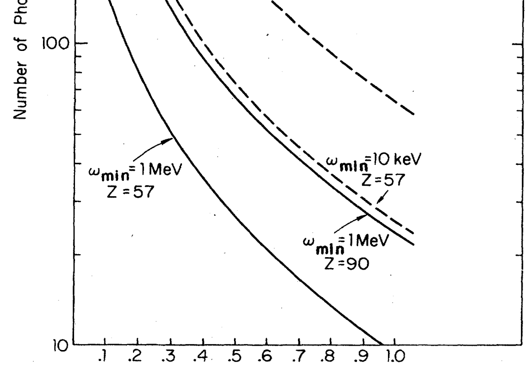

FIG. 5. Total photon yields for nuclei with $Z=57$ and $Z=90$ for various values of the parameter a.

If the distribution of photons of momentum $\vec{k}$ emitted from a π^0 meson of momentum $\vec{p}$ is $dN(\vec{p},\vec{k})/d^3k$, then the distribution of photons is

$$\frac{dN^\gamma}{d^3k}=\int d^3p\frac{dN^\pi}{d^3p}\frac{dN(\vec{p},\vec{k})}{d^3k} . \tag{20}$$

The distribution of photons is isotropic in the pion rest frame and two photons are emitted per decay, so that the pion-photon distribution is

$$\frac{dN}{d^3k_1d^3k_2}=\frac{1}{\pi|k_1||k_2|}\delta^{(4)}(p-k_1-k_2) , \tag{21}$$

where $\vec{k}_1$ and $\vec{k}_2$ are the two photon momenta. The distribution of photons becomes

$$\frac{dN^\gamma}{d^3k}=\int d^3p\frac{1}{E}F\left[\frac{E-p}{M_p}\right]g(p_T)\frac{1}{\pi|\vec{k}||\vec{k}-\vec{p}|}\times\delta(E-|\vec{k}|-|\vec{k}-\vec{p}|) . \tag{22}$$

The roots of the δ function are given by

$$|\vec{k}|=\frac{m_\pi{}^2}{2}(E-\vec{p}\cdot\hat{k})^{-1} . \tag{23}$$

For very soft photons $|\vec{k}|\ll m_\pi$, this equation becomes

$$p=\pm\frac{m_\pi{}^2}{2k}(1\mp\cos\theta)^{-1} . \tag{24}$$

The negative solution arises from photons which become Doppler shifted when emitted from pions which are moving against the beam direction in the target frame. Since there are not many such pions, this contribution is suppressed relative to those which are Doppler shifted when pions move forward. For very-low-frequency photons, the pion must move very fast along the beam direction in order to generate a large enough Doppler shift. The source of background soft photons is therefore primarily central-region pions.

The integrals are now straightforward to perform so that

$$\frac{dN^\gamma}{d\omega\,d\Omega}=\frac{2}{\pi}\left[\frac{\omega}{m_\pi}\right]^2\frac{dN}{dy}\bigg|_{y=0} . \tag{25}$$

Notice that this background is isotropic, as distinguished from the bremsstrahlung photons which are forward peaked. This is modified somewhat by the next-higher-order corrections.

To estimate this background, recall that for pp collisions the central-region multiplicity of charged pions is $dN/dy\cong2$. For neutral pions in a nucleus-nucleus collision, we conservatively take

$$\frac{dN}{dy}\bigg|_{\pi^0,y=0}=(1-4)A . \tag{26}$$

For $\omega_{\max}<20$ MeV for all values of a, the background is smaller than the signal. For $Z=90$, and for $a=1$, the background is 50% of the signal at $\omega=15$ MeV. For $a=0.3$, the ratio is 10%.

IV. SUMMARY

The emission of bremsstrahlung photons in ultrarelativistic nuclear collisions provides a means of measuring the impact-parameter and velocity distributions of final-state nucleons. These measurements must be performed at small angles, and must be capable of detecting relatively soft photons. The backgrounds due to π^0 photons appear to be small for photons which have $\omega<15$ MeV in the target nucleus rest frame.

There are three separate kinematical situations where these photons might be experimentally studied. In fixed-target experiments, either the target fragmentation region or the projectile fragmentation region might be studied. In the target fragmentation region, the photons of interest are soft and typically have frequencies $\omega<15$ MeV. Such photons are emitted in a fairly wide angular region in the hemisphere along the direction of the projectile's momentum. Another kinematic region is the projectile fragmentation region. For a projectile with $E/A=200$ GeV/nucleon, the photons of interest have frequencies $\omega<3$ GeV, and are emitted in a small angular region of spread of order 1–10 mrad. For a collider of $E/A=30$ GeV/nucleon, the photons have frequencies of $\omega<0.5$ GeV and are in small angular regions spread ~10 mrad around the direction of motion of the colliding nuclei.

ACKNOWLEDGMENT

L. McLerran thanks J. Kapusta for useful discussions.

APPENDIX A: THE ANGULAR-DISTRIBUTION FUNCTION

The angular-distribution function $g(\theta)$ is given by Eq. (9) as

$$g(\theta)=a\sin\theta\int dy\,e^{-ay}\frac{v(y)}{1-v(y)\cos\theta} . \tag{A1}$$

With

$$u=e^{-2y} \tag{A2}$$

this integral becomes

$$g(\theta)=\frac{a}{2}\sin\theta\int_0^1du\,u^{-1+a/2}(1-u)\left[1+u\frac{1+\cos\theta}{1-\cos\theta}\right]^{-1} . \tag{A3}$$

Using the integral representation for the hypergeometric function,

$$\int_0^1du\,u^{\beta-1}(1-u)^{\gamma-\beta-1}(1-uz)^{-\alpha}=\frac{\Gamma(\beta)\Gamma(\gamma-\beta)}{\Gamma(\gamma)}{}_2F_1(\alpha,\beta;\gamma;z) \tag{A4}$$

we find

$$g(\theta)=\frac{a\sin\theta}{(1-\cos\theta)}\frac{1}{1+a/2}{}_2F_1\left[1,\frac{a}{2};\frac{a}{2}+1;-\frac{1+\cos\theta}{1-\cos\theta}\right] . \tag{A5}$$

The argument of this function is not between 0 and 1, and is not expandable in a convergent Taylor-series expansion. To correct this we use

$$ {}_2F_1(\alpha,\beta;\gamma;z)=(1-z)^{-\alpha}\frac{\Gamma(\gamma)\Gamma(\beta-\alpha)}{\Gamma(\beta)\Gamma(\gamma-\alpha)}{}_2F_1\left[\alpha,\gamma-\beta;\alpha-\beta+1;\frac{1}{(1-z)}\right] $$
$$ +(1-z)^{-\beta}\frac{\Gamma(\gamma)\Gamma(\alpha-\beta)}{\Gamma(\alpha)\Gamma(\gamma-\beta)}{}_2F_1\left[\beta,\gamma-\alpha;\beta-\alpha+1;\frac{1}{(1-z)}\right] \tag{A6} $$

to find

$$ g(\theta)=\sin\theta\left[\frac{1}{(a-2)}{}_2F_1\left[1,2;2-\frac{a}{2};\frac{(1-\cos\theta)}{2}\right]\right. $$
$$ \left.+(1-\cos\theta)^{a/2-1}2^{-a/2-1}\frac{a\pi}{\sin(a\pi/2)}{}_2F_1\left[\frac{a}{2},\frac{a}{2}+1;\frac{a}{2};\frac{(1-\cos\theta)}{2}\right]\right]. \tag{A7} $$

This function exhibits the singular behavior

$$ g\to\frac{a\pi}{2^a\sin(a\pi/2)}\theta^{a-1} \tag{A8} $$

for $\theta\to 0$. The function is nonsingular at $\theta=\pi$. To see this, use the identities

$$ {}_2F_1(\alpha,\beta;\gamma;z)=\frac{\Gamma(\gamma)\Gamma(\gamma-\alpha-\beta)}{\Gamma(\alpha)\Gamma(\beta)}{}_2F_1(\alpha,\beta;\alpha+\beta-\gamma+1;1-z) $$
$$ +(1-z)^{\gamma-\alpha-\beta}\frac{\Gamma(\gamma)\Gamma(\alpha+\beta-\gamma)}{\Gamma(\alpha)\Gamma(\beta)}{}_2F_1(\gamma-\alpha,\gamma-\beta;\gamma-\alpha-\beta+1;1-z) \tag{A9} $$

and

$$ {}_2F_1(a,b;b;z)=(1-z)^{-a} \tag{A10} $$

to conclude

$$ g(\theta)=\frac{a\sin\theta}{a+2}{}_2F_1\left[1,2;2+\frac{a}{2};\frac{(1+\cos\theta)}{2}\right]. \tag{A11} $$

APPENDIX B: THE BACKGROUND FROM π^0 DECAYS

We begin with Eq. (24):

$$ \frac{dN^\gamma}{d^3k}=\int d^3p\frac{1}{E}F\left[\frac{E-p}{M_p}\right]g(p_T)\frac{1}{\pi|\vec{k}||\vec{k}-\vec{p}|}\delta((p^2+m^2)^{1/2}-|\vec{k}|-|\vec{k}-p|). \tag{B1} $$

For soft photons, we evaluate the zero of the δ function at large p as

$$ p\sim\frac{m_\pi{}^2}{2k(1-\cos\theta)}-\frac{km_T{}^2}{m_\pi{}^2}+p_T\frac{\sin\theta\cos\phi}{1-\cos\theta}. \tag{B2} $$

Since

$$ \frac{\partial}{\partial p}(E-|k|-|k-p|)\sim-\frac{kp(1-\cos\theta)}{E|k-p|}\left[1-2k^2\frac{m_T{}^2}{m_\pi{}^4}\cos\theta(1-\cos\theta)\right] \tag{B3} $$

and

$$ \frac{(E-p)}{M_p}\sim m_T{}^2k\frac{(1-\cos\theta)}{m_\pi{}^2M_p} \tag{B4} $$

the integral becomes

$$ \frac{dN^\gamma}{d\omega\, d\Omega}=\frac{1}{\pi}\int dp\, d^2p_TF\left[\frac{m_T{}^2k(1-\cos\theta)}{m_\pi{}^2M_p}\right]g(p_T)\frac{1}{p(1-\cos\theta)(1-2k^2m_T{}^2\cos\theta(1-\cos\theta)/m_\pi{}^4)} $$
$$ \times\delta\left[p-\frac{m_\pi{}^2}{2k}(1-\cos\theta)^{-1}-\frac{km_T{}^2}{m_\pi{}^2}+p_T\frac{\sin\theta\cos\phi}{(1-\cos\theta)}\right]. \tag{B5} $$

Evaluating the δ function and expanding in small k, we find

$$\frac{dN^\gamma}{d\omega\, d\Omega}=\frac{2}{\pi m_\pi^2\omega}\int d^2p_T F\left[m_T^2 k\frac{(1-\cos\theta)}{m_\pi^2 M_p}\right] g(p_T)(1+2k^2m_T^2\sin^2\theta/m_\pi^4+4p_T^2k^2\sin^2\theta\cos^2\phi)$$

$$=\frac{2}{\pi m_\pi^2\omega}\frac{dN}{dy}\bigg|_{y=0}\left[1+\frac{4k^2\langle p_T^2\rangle}{m_\pi^4}\sin^2\theta\left[\frac{F(k\langle p_T^2\rangle(1-\cos\theta)/m_\pi^2M_p)}{F(0)}-1\right]\right]. \tag{B6}$$

The yield of photons is therefore

$$\left\langle\frac{dN^\gamma}{d\omega\, d\Omega}\right\rangle=\frac{2}{\pi m_\pi^2\omega}\frac{dN}{dy}\bigg|_{y=0}\left\{1+\frac{2k^2\langle p_T^2\rangle}{m_\pi^4}\{[F(k\langle p_T^2\rangle/m_\pi^2M_p)/F(0)-1]\}\right\}. \tag{B7}$$

[1] J. Kapusta, Phys. Rev. C **15**, 1580 (1977).
[2] M. P. Budinsky, S. P. Ahlen, G. Tarle, and P. B. Price, Phys. Rev. Lett. **49**, 361 (1982).
[3] J. D. Jackson, *Classical Electrodynamics* (Wiley, New York, 1962), pp. 505ff.